ROYAL SOCIETY
OF CHEMISTRY

PAPER

Check for updates

Solvatochromism in SWCNTs suspended by conjugated polymers in organic solvents†

Andrzej Dzienia, [ID] *[a,b] Dominik Just[a] and Dawid Janas [ID] *[a]

Despite the extensive utilization of carbon nanostructures as sensors, the factors that most affect their performance remain insufficiently understood. Many nanocarbon-based sensors are either processed in liquid environments or applied as liquid suspensions, which leads to solvatochromism, substantially influencing the underlying optical transitions. Most of the principles established so far apply only to nano-carbon species dispersed in polar environments by common surfactants, so the reported findings are not universal. For instance, they cannot describe the behavior of single-walled carbon nanotubes (SWCNTs) suspended in organic solvents by conjugated polymers (CPs), which have recently received considerable attention from the scientific community. Our research responds to this lack of knowledge and provides a thorough understanding of this topic by investigating SWCNT nanocomposites based on polyfluorenes and their co-polymers. A careful selection of an autonomous reference and precise spectral analysis allowed us to measure absolute solvatochromic shifts, by using which we identified and derived the underlying relationships affecting the optical properties of the material. Elucidation of the complex inter-actions between the polymer structure, SWCNT chirality, and solvent characteristics gave rise to the for-mulation of a revised mechanism of solvatochromism in SWCNTs. The in-depth experimental and theore-tical examination revealed that in the case of CP-solubilized SWCNTs, the solvatochromic shifts strictly depend on the assignment of individual chiral types to mods and families, which experience the strain exerted by the polymer chains in different ways.

1. Introduction

Ever since their discovery, single-walled carbon nanotubes (SWCNTs) have been of interest to numerous scientists because of their unique electrical,[1] mechanical,[2] optical,[3] and other[4,5] properties. Nowadays, the photonic characteristics of SWCNTs are of particular interest as they open new research avenues in such distant fields as telecommunications,[6] cryptography,[7] and medical diagnostics.[8] Because many types of SWCNTs have their characteristic absorption or emission bands in the range of the so-called tissue transparency window, they can be employed to study biological materials or even the functioning of living organisms.[9] Many previous studies have capitalized on the fact that the properties of SWCNTs are highly susceptible to their surrounding microen-vironments, giving rise to their application as nanosensors.[8,10] Considering the recent discovery that chemical modification

can significantly enhance the photonic characteristics of SWCNTs,[11] their commercial deployment as sensors or light emitters appears imminent.

However, the sensitivity of optical properties to the appli-cation conditions is a double-edged sword, which simul-taneously hampers their broad-scale implementation. In many cases, the atmosphere (air/vacuum; humidity), solvent (aqueous/organic), dispersing agent (surfactant/polymer), *etc.*, strongly affect the nature of SWCNTs. Unfortunately, the impact of these factors on the optical properties of monochiral SWCNTs remains largely unresolved. Admittedly, reaching a thorough understanding of the behavior of the optical pro-perties of SWCNTs and the mechanisms of light emission/absorption is non-trivial due to the complexity of the subject. The lack of satisfactory progress on this front likely stems from the fact that many chirality-defined SWCNT fractions are still unobtainable or only available in low amounts.[12] Hence, opportunities for their analysis are limited.

Despite these challenges, researchers have studied how the optical properties of SWCNTs change in several quite distinct situations. Initially, the experiments were focused on individual CNTs suspended between pillars[13] or trenches.[14] However, as confirmed by other studies,[15] it was determined that the positions of the observed E_{11} and E_{22} transitions strongly

[a]*Department of Chemistry, Silesian University of Technology, B. Krzywoustego 4, 44-100 Gliwice, Poland. E-mail: Andrzej.Dzienia@polsl.pl, Dawid.Janas@polsl.pl*
[b]*Institute of Materials Engineering, University of Silesia in Katowice, Bankowa 12, 40-007 Katowice, Poland*
†Electronic supplementary information (ESI) available. See DOI: https://doi.org/10.1039/d3nr00392b

depend on the induced mechanical stresses and contact with the surface. Moreover, it was noted that vacuum experiments do not consider solvatochromism induced by the adsorption of molecules,[16] which occurs in real-life conditions. Hence, despite the merits of these pioneering investigations, analysis in artificial environments devoid of gases or solvents is of limited relevance for practical applications. Consequently, many research groups reoriented attention to inspecting SWCNTs suspended in liquid media.[17–25]

To understand the behavior of solubilized SWCNTs, it is first necessary to individualize them in the liquid medium since interactions between individual SWCNTs strongly affect the optical transitions.[26,27] For this purpose, dispersing agents such as surfactants[12] or conjugated polymers (CPs)[28–32] (with a preference for aqueous and organic environments, respectively) that break up SWCNT bundles, thereby producing isolated SWCNTs in solution, can be applied. Unfortunately, the influence of the latter group of agents on the optical properties of SWCNTs under polar/non-polar solvent conditions is only vaguely understood.

To date, most studies have focused on the analysis of SWCNTs dispersed by surfactant molecules in water,[17–20] optionally with molecules of organic solvents injected into micelles, which arrange themselves at the interface of the SWCNT sidewall and the hydrophobic part of the surfactant.[25] Based on the recorded data, solvatochromic shifts were found to follow values of solvent-induced polarization. Nevertheless, this approach did not eliminate the influence of water, as some of the SWCNT surface can still be exposed to the aqueous environment, giving a limited insight into the impact of the microenvironment on the optical characteristics of SWCNTs.

As a solution to this problem, Stranks and colleagues employed porphyrin oligomers able to disperse SWCNTs in non-aqueous media.[33] Similarly, Choi *et al.* used flavin derivatives (FC12 or FMN) that were compatible with several organic solvents and water.[22] Both teams obtained valuable findings explaining how the solvent and the dispersant affect the optical properties of SWCNTs. However, neither the porphyrins nor flavins afforded monochiral SWCNT fractions, so a precise analysis of how chirality-defined SWCNTs are affected by their microenvironment remains out of reach.

Shortly after the discovery that CPs can extract monochiral SWCNTs[34,35] (or provide remarkable enrichment with selected SWCNT types[12]) in a broad spectrum of organic solvents, their application potential increased at a staggering pace. Therefore, polymer-dispersed SWCNTs, which are available in various media, are highly applicable for studying the phenomenon of solvatochromism. Although the solubilization mechanism exhibited by polymers differs from that of typical small-molecule surfactants, they also provide material whose properties are sensitive to the environment.[33,36] While trying to solubilize SWCNTs, it was noted that a range of parameters of dispersants and solvents, such as dielectric constant, polarizability, number of donor/acceptor groups, and the presence of π-planes, strongly impact the optical properties of SWCNTs.[21–25]

In the case of polymers, several additional factors must also be considered due to the much more complex solubilization mechanism and the influence of the chain length (molecular weights). As highlighted by modeling, these macromolecules can coat SWCNTs in various ways through a straight, helical, or disordered arrangement of polymer molecules on the SWCNT surface,[37,38] which is considerably less straightforward than the simple deposition of surfactant molecules. Meanwhile, commonly present side chains in the polymers can also "lock" the formed structure by additional wrapping and/or interact with other side chains, polymer chains, SWCNTs, or solvent molecules.[38,39] Furthermore, in some cases, depending on the polymer type, its concentration, and the type of SWCNT, multiple polymer layers can be deposited on the surface, which can substantially change the perceived nature of the SWCNT.[39]

Because the behavior of a given system depends on the chirality of the selected SWCNTs and "molecular matching" of the polymer, the relevance of particular trends is not universal for the entire population of SWCNTs but is valid only for specific subsets of them.[21,22,24] Furthermore, another level of complexity, which is rarely considered due to computational challenges, is induced by the fact that solvents, in addition to directly affecting SWCNTs in areas not covered by the polymer, also alter the conformation of the polymer's scaffold and side chains, its stiffness, as well as its alignment on the surface of SWCNTs.[21,38,39] In turn, the rigidity of the polymer chains affects the potential for the induction of mechanical stresses, which can strongly impact the energy levels of optical transitions.[33] Lastly, CPs themselves can strongly influence the properties of SWCNTs as they form numerous π–π interactions with them, as opposed to surfactants which mainly interact with SWCNTs through weak hydrophobic interactions. Regrettably, the above effects have only been observed on a limited number of SWCNT/polymer/solvent systems in separate studies, so it has not been possible to draw precise and comprehensive conclusions.

In this study, we compiled the knowledge available in the literature about the position of the E_{11} and E_{22} transitions for multiple SWCNT chiralities in both water and organic solvents. We demonstrated how the optical absorption of SWCNTs suspended non-selectively by PFO-T co-polymers (of various molecular weights and ratios of polymer to SWCNTs) can be interpreted to elucidate the underlying phenomena affecting SWCNT photonics. In the next step, we introduced a new approach to studying solvatochromic shifts of SWCNTs in various media. The concept we developed unlocks the possibility of analysis of the optical properties of near-monochiral (6,5) and (7,5) SWCNTs extracted with PFO-BPy and PFO, respectively. Based on the obtained results, correlated with various solvent parameters such as dielectric constant, dipole moment, and polarizability, we provide a complete picture of the solvatochromic effect in SWCNTs suspended with CPs in organic solvents, which are currently broadly employed to manufacture SWCNT-based devices for optoelectronics. We reveal that the solvatochromic shifts experienced by SWCNTs

suspended in organic solvents are highly affected by the strain exerted by the polymers used to disperse them. Interestingly, the magnitude of this effect can be predicted by considering the specific family to which a particular SWCNT belongs.

2.   Experimental

2.1.   Materials

All chemical reagents and solvents (Table S1†) were used as supplied, without additional purification or drying (except when stated otherwise). The purity of the reagents, along with the manufacturer and data allowing identification of the products, can be found in the ESI.† The experiments were carried out with HiPco SWCNTs (NanoIntegris, lot: HP30-006) and CoMoCAT (6,5)-enriched SWCNTs (Sigma-Aldrich, lot: MKCM5514).

2.2.   Polymer synthesis

The syntheses of PFO-T, PFO, and PFO-BPy (6,6′) were carried out using the Suzuki coupling procedure (Fig. 1). Two batches with different molecular weights of PFO-T were produced. The structures of the polymers were confirmed by ^{1}H NMR spectroscopy (Fig. S1–S3†). The macromolecular parameters were examined by SEC and listed in Table S2.†

2.3.   Preparation of SWCNT dispersions

In a typical dispersion process, 1.5 mg of the selected SWCNTs and 6 mg of polymer were weighed into two 13 mL glass vials. Next, the polymer was dissolved in 4 mL of a solvent chosen from those listed in Table S1† under ambient conditions. The polymer solution was transferred to the second vial, which contained the pre-weighed SWCNTs. The mixture was homogenized in an ice-cooled ultrasonic bath for 30 minutes (Polsonic, Sonic-2, 250 W). Sonication was then carried out with a tip sonotrode for 8 min at 30 W (Hielscher UP200St ultrasonic generator) to disentangle the SWCNTs and wrap the polymers around them. After sonication, the thick suspension was transferred to 5 mL conical tubes and centrifuged at 10 000 rpm (15 314g) for 5 minutes to remove the bundled SWCNTs and polymer aggregates. Finally, 90% of the supernatant was transferred to a fresh vial and analyzed by spectroscopy.

2.4.   Absorption spectroscopy

Optical absorption spectra were recorded immediately after centrifugation, in a range of 400–1100 nm using a Hitachi U-2910 spectrophotometer and in a range of 400–1700 nm using a PerkinElmer Lambda 1050 spectrophotometer. A double beam mode was used with a pure solvent cuvette placed in the reference channel. The background was removed from the spectra by means of asymmetric least squares smoothing (ALSS) using OriginPro 2022.[40] Finally, the data was normalized to a range of 0 to 1 to facilitate comparison between samples, which is a standard procedure.[41]

2.5.   Deconvolution of absorption spectra

Deconvolution was performed using the Voigt function with the PTF Fit application.[42] Due to the large red shifts between the observed peak positions in organic solvents and the values determined by Weisman in D_2O,[43] it was necessary to tune the reference file to enable accurate peak fitting. The generated peak positions for a broad spectrum of SWCNTs were used for the analysis.

3.   Results and discussion

3.1.   State of the art

During our research on sorting SWCNTs, we noticed that it was difficult to identify a wavelength at which the characteristic S_{11} and S_{22} transitions could be monitored, especially for
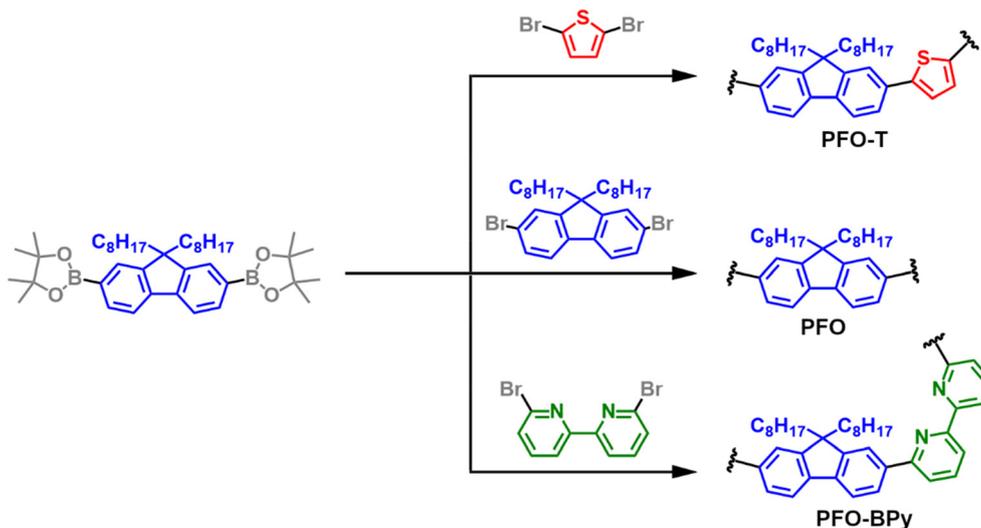

Fig. 1   Synthetic approaches used to obtain PFO-T, PFO, and PFO-BPy.

less popular SWCNTs such as (6,4) or (7,3). Although there are theoretical and experimental data acquired by extensive study of the photonic characteristics of SWCNTs, these mostly encompass dry SWCNTs (kept in vacuum or air) or those solubilized in water using surfactants such as SDS or DOC.[17,19,43] Moreover, the published results are not entirely coherent as different groups process the SWCNTs dissimilarly using various solubilizing agents, system compositions, or solvents, which sometimes leads to misleading discrepancies. Consequently, the impact of the microenvironment on the electrical properties of polymer-wrapped SWCNTs has not been elucidated. The differences in peak position measured at two extremes, such as SWCNTs solubilized with a weak surfactant in water or by poly(thiophene) in a halogenated aliphatic solvent, can be as high as 100 nm.[39,43] This issue is particularly problematic when several chiralities have fingerprints across a narrow spectral area. For instance, between 800 and 1060 nm, E_{11} signals from (5,4), (6,4), (9,1), (8,3), (6,5), (7,3), (7,5), and (8,1) can be detected. The spectral congestion is even more troubling in the case of E_{22} transitions, the intensity of which can additionally be affected by the presence of metallic SWCNTs, which absorb in this range. Absorption spectroscopy is commonly used for its simplicity and reliability, so it would be indispensable to have an accurate dataset for SWCNTs of different chiralities, suspended in various solvents using several dispersing agents.

Considering the above concerns, we decided to collect the available literature data to show statistically where peak positions from individual chiralities can be found, either in aqueous or organic media (Fig. 2). In the latter case, the transitions occurred at higher wavelengths, as visualized by the median values included in the plot. Moreover, although the range of results for SWCNTs suspended with polymers in organic solvents was often broader, the median results accurately described the peak positions of the most abundant SWCNTs arising from harvesting carried out by typical poly-

fluorenes and their co-polymers, e.g., (6,5) at 992 nm or (7,5) at 1042 nm (within 10 nm confidence range). However, determining reliable and accurate values for the few remaining chiralities, which are less common in raw SWCNT materials, is a problem. Consequently, their optical properties have been reported only sporadically, and the findings come from many papers in which isolation was carried out under different conditions, so their comparison is questionable.

3.2. Methodology employed to quantify solvatochromism

To tease out the role of the environment on the optical properties of SWCNTs, we decided to employ two parallel approaches. The first focused on a single CP, which can suspend a broad range of chiralities, and unsorted HiPco SWCNTs. The motivation was to find out if it was possible to build a robust protocol for analyzing solvatochromism in nanocarbon materials of complex composition. Based on extensive preliminary studies including a variety of fluorene co-polymers, we synthesized and employed a thiophene-based polymer (alternating co-polymer of 9,9-dioctylfluorene with thiophene (PFO-T)), which provided extensive solubilization capabilities to a broad range of SWCNTs due to its non-selective affinity toward SWCNTs. By using a single polymer, we were able to interpret the effect of solvent on the optical properties of SWCNTs, eliminating interference such as structure (type of repeatable units, nature of end groups, length of side chains, etc.), batch-to-batch variations, and processability that commonly distort the conclusions reported in the literature.

In contrast, the second approach was intended to analyze a source material with a smaller number of different chiralities, i.e., CoMoCAT, and two selective CPs, PFO-BPy and PFO, redirecting the focal point to the influence of the polymer. Their structural differences (types of subunits, presence of heteroatoms with free electron pairs) and spatial conformation enabled selective isolation of (6,5) and (7,5) chiralities, respectively, for examination. Armed with the knowledge of the posi-
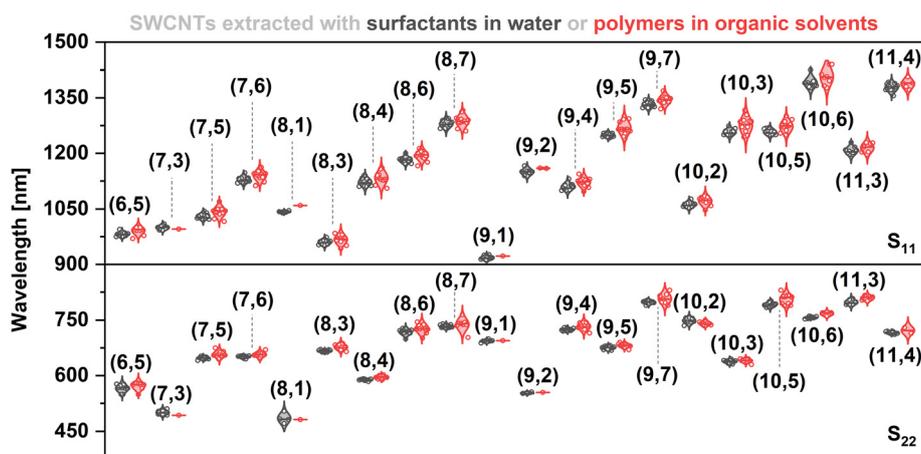

Fig. 2 Peak maxima of S_{11} and S_{22} transitions of SWCNTs suspended by surfactants in water and polymers in organic solvent (toluene), obtained from optical data reported in the literature.[21,24,44–51] Straight horizontal lines mark the median values. The median, lowest, and highest reported values for each chirality are reported in Table S3.†

tion of the peaks from the abovementioned chiralities, stemming from the results for all the polymers tested in toluene, we were able to gain insight into how the structure of the polymer translated into the strength of the solvatochromism effect.

3.3. Non-selective extraction of SWCNTs with PFO-T

Conjugated polymer extraction (CPE), carried out on HiPco using the non-selective polymer PFO-T, demonstrated, as we expected, that this polymer exhibited a remarkable ability to solubilize the entire spectrum of chiralities available in the source material, as illustrated in Fig. S4.† In addition, the sharp shape of the peaks indirectly shows that the SWCNTs were well individualized. The observed outcome may be explained by the localization of a strong charge in the form of two free electron pairs on the sulfur atom placed in a ring smaller than a typical six-membered one, as well as significant flexibility in terms of possible chain conformations. The latter aspect is very complex in the case of CPs, which are commonly characterized by a limited ability to rotate around the bonds between moieties, contrary to classical polymers linked with single, nonconjugated bonds.[52] Conventionally, the CPs used for selective extraction of SWCNTs have bulky subunits, making them a relatively rigid scaffold with limited molecular alignment, preferably only available for a single chirality.

On the contrary, the employed polyfluorene-alt-thiophene has more degrees of freedom compared to fluorene-based homopolymers,[53] which explains why it can bind to numerous SWCNTs with different chiral angles and diameters.[54] One parameter that gauges the applicability of a given polymer for SWCNT solubilization is the persistence length, which quantifies a polymer's flexibility. For instance, if the total length of the polymer chain is shorter than its persistence length, it behaves like a rigid rod.[55,56] Polythiophenes (and consequently alternating co-polymers of fluorene and thiophene) have a shorter persistence length than polyfluorenes due to the lower number of fused aromatic rings, which facilitates their ability to establish a molecular match to a wider range of nanotube types with lower dependency on their diameter and chiral angle. It is also relevant that the applied thiophene moiety does not contain side chains, so the rotation around the bond between the subsequent subunits is essentially unhindered.[57]

Regarding SWCNT individualization, the capabilities of the fluorene-alt-thiophene co-polymer on this front were exceptionally promising. As shown by the provided spectra, PFO-T offered much better individualization in organic solvents compared to perhaps the best surfactant utilized for the dispersion of SWCNTs in water, which is sodium deoxycholate (DOC) (Fig. S4a†). This ability was likely the result of near-complete SWCNT debundling, which translated into much narrower absorption peaks from individual chiralities, and, consequently, a much higher peak-to-valley ratio (better signal separation from specific nanotube types), which was crucial for accurate deconvolution. This enhancement of spectral "resolution" motivated us to perform a more thorough analysis of the suspension composition by deconvolution of the absorption

spectra using multiple peak fitting with Voigt functions. Fig. S4b† shows the deconvolution results, which gave high agreement between the simulated and experimental data. The expected SWCNT types were accurately represented, and the discrepancy between the recorded and simulated absorption curves was negligible.

Since we were satisfied with these results, we extended the analysis to probe the effect of molecular weight on the yield and selectivity of CPE. For this purpose, we synthesized PFO-T of lower molecular weight and carried out an analogous harvesting process (Fig. S4a†). We did not observe any significant differences between the suspensions obtained from the two investigated batches of PFO-T. Another important factor to consider was the weight ratio of polymer to SWCNT. In the case of a selective polymer such as PFO, this ratio is crucial to achieving a decent degree of individualization and, most importantly, a high chiral purity of the suspension (Fig. S5†). We investigated this aspect in the case of non-selective PFO-T by carrying out CPE using four different weight ratios of polymer to SWCNTs, i.e., from 3 : 1, through 4 : 1 and 6 : 1, up to 8 : 1. Remarkably, also in this case, we did not note any significant effect of the studied weight ratio on the shape of the absorption spectra for each experiment (Fig. S6a†).

To understand this observation, it is helpful to consider the results published by Stranks et al., who studied the process of the polymer deposition on the SWCNT surface. The authors analyzed the deposition of two polymers onto SWCNTs in chlorobenzene, i.e., poly(3-hexylthiophene-2,5-diyl) (P3HT) and poly(9,9-dioctylfluorene-alt-benzothiadiazole) (F8BT).[39] They found that P3HT, unlike F8BT, cannot form multi-layer systems. Despite this, SWCNTs wrapped with P3HT were characterized by a powerful shift in peak position toward higher wavelengths with respect to other studied CPs. How strong this effect was can be seen from the fact that the S_{11} transition for polythiophene-dispersed SWCNTs originating from (6,5) chirality was observed at 1021 nm, while for (8,4) it was noted at 1141 nm, whereas the equivalent values for F8BT were 998 and 1133 nm, respectively.[39]

In the case of polythiophenes, an even greater shift was caused by the formation of a thicker shell where polymer excess was practically restricted, in contrast to F8BT, for which a constant and linear shift in peak position was evident due to its ability to create multiple layers on the surface of SWCNTs.[39] The dielectric shielding in polythiophene (even for a single polymer layer) was strong because (i) the polymer covered the SWCNT surface well due to its high flexibility, and (ii) its electronic characteristics were favorable, leading to energy transfer caused by the overlap of the energy bands of the polymer and the SWCNTs.[36,39,54] Conversely, the bulkiness of F8BT polymers and their reduced ability to rotate their units left some of the space on the SWCNT uncovered. Adding another layer of polymer on top could deposit on these bare SWCNT portions, thereby causing a shift in the optical transition peaks. Nonetheless, the shifts observed for F8BT were less notable due to the large bandgap, which was non-optimal for the suspended SWCNTs. Interestingly, the polymer deposition kine-

tics were influenced by the chirality of the SWCNTs. In the case of P3HT, the coating was most immediate for (8,4), (7,5), and (8,3) SWCNTs, while near-armchair chiralities, *i.e.*, (6,5) and (7,6), required more time or larger polymer : SWCNT ratios.

Based on the described insight, it might be anticipated that the lower share of the thiophene moiety in each repetitive unit of PFO-T used by us (with respect to the P3HT) should give rise to a moderate impact on the optical properties of SWCNTs, while likely keeping the effect stronger than for stiff fluorene-based homopolymers. The alternating presence of thiophene subunits makes the polymer more flexible, so it can better wrap around the SWCNTs than rigid PFO or PFO-BPy. Simultaneously, the formation of a PFO-T multi-layer on SWCNTs can be ruled out as the modification of molecular weight of the polymer or the ratio of polymer to SWCNT induced only slight changes to the absorption spectra (Fig. S6†). Thus, it can be concluded that the PFO-T co-polymer behaved predominantly like regular polythiophene, which is highly flexible but cannot form multi-layer composites with SWCNTs.[39]

In this complex discussion, it is easy to overlook the role of the solvent utilized in the abovementioned manuscript, namely, chlorobenzene. This particular solvent has a higher ability to solvate CP, which may increase the tendency to form multi-layer systems in contrast to the toluene employed herein. Even though toluene is almost exclusively used in CPE, it is a non-optimum solvent from the CP point of view. While this solvent keeps CPs rigid, which is necessary for chirality-oriented selectivity, it decreases the flexibility of the polymer chains, reducing their ability to form multi-layer polymer/ SWCNT systems. Consequently, solvatochromic shifts in this medium are more challenging to discern.

To quantitatively confirm the observations concerning the lack of a notable spectral shift, the obtained spectra from SWCNTs suspended using various amounts of PFO-T were deconvoluted to separate signals from individual SWCNTs. Subsequently, the peak positions from the generated data were extracted for all selected polymer/SWCNT ratios and summarized in Fig. S6b.† The differences between the maxima of the S_{11} peaks were negligible and not statistically significant in most cases. The discrepancy between samples appeared highest for SWCNTs that were present in low amounts, such as (11,7), (6,4), (9,4), and (8,4), which are difficult to fit with high precision when a polydisperse SWCNT mixture is analyzed. These differences covered all possible sources of measurement uncertainty, not only those originating from the user and the apparatus, but also fluctuations in the surface coating formed by the polymer and fitting errors.

Despite the introduction of such measurement uncertainty, the small standard deviations indicated that the PFO-T-guided CPE was highly robust to changes in the composition of the system and the conditions of the SWCNT suspension. This fact was crucial for our further studies because it enabled us to speculate with a high degree of confidence that the subsequently reported solvatochromic shifts were predominantly

caused by the change of microenvironment around the SWCNTs. For the next experiments, we chose a ratio of 4 : 1 as it presented a sufficiently high optical density, while the amount of utilized polymer was minimal. This condition was important as, ideally, we wanted to expose the maximum amount of SWCNT surface to the solvent molecules, so they affected the optical properties of the SWCNTs. At the same time, we needed to ensure the stability of the SWCNT dispersion, so the polymer content could not be too low.

To examine the solvatochromism effect induced by PFO-T, it was necessary to perform a series of CPE in various solvents differing in polarity, dielectric constant, and the ratio of aliphatic to aromatic moieties (Fig. 3a). Although SWCNTs can be dispersed in a wide spectrum of both polar and non-polar solvents, the limiting factor in the scope of this study is the compatibility of the polymer with the liquid medium. Non-polar aprotic solvents such as toluene and xylene promote high selectivity of extraction through CPE,[35,58,59] while the polar ones such as tetrahydrofuran usually tend to show a reduction in selectivity.[60] Besides, the use of more polar protic solvents requires polymers with modified side chains to make them soluble.[61] Keeping in mind these guidelines and the results of preliminary studies, we chose benzene, tetralin, and anisole as hydrophobic solvents with low and high dielectric constants, $\varepsilon = 2.28$, $\varepsilon = 2.77$, and $\varepsilon = 4.3$, respectively, and hydrophilic solvents differing greatly with respect to this variable, *i.e.*, tetrahydrofuran and dimethylformamide with $\varepsilon = 7.6$ and $\varepsilon = 36.7$, respectively. In addition to this quite broad array of solvents, we also selected toluene, *m*-, and *o*-xylene as environments very commonly used in CPE. Our selection was limited in this regard by the compatibility of the CPs, which for certain polar solvents completely lose their ability to individualize SWCNT or form very unstable suspensions. A summary of the chosen parameters of each tested solvent is provided in Table S1.†

Analysis of the absorption curves in Fig. 3b indicates that an acceptable level of individualization was achieved in all cases. Moreover, the suspension selectivity of PFO-T was much more responsive to solvents than to either the molecular weight of the polymer or the weight ratio. Before we move on to a thorough discussion of the effects of solvatochromism depicted in Fig. 3b and c (given in Section 3.5), for the sake of clarity of the entire work, we would like to present the second approach that we devised, which was based on the PFO and PFO-BPy selective polymers (the structures of which are depicted in Fig. 1), to fully understand the solvatochromic effect of SWCNTs suspended by various polymers in organic solvents.

3.4. Selective extraction of SWCNTs with PFO-BPy and PFO

We aimed to minimize the influence of the solvent upon the polymer conformation and, thus, the selectivity of the CPE. To highlight the importance of this issue, we first performed a series of isolations from CoMoCAT (6,5)-enriched SWCNTs by PFO in benzene and toluene, and the outcomes are compiled in Fig. S7a† (results for PFO-T used in the previous section for
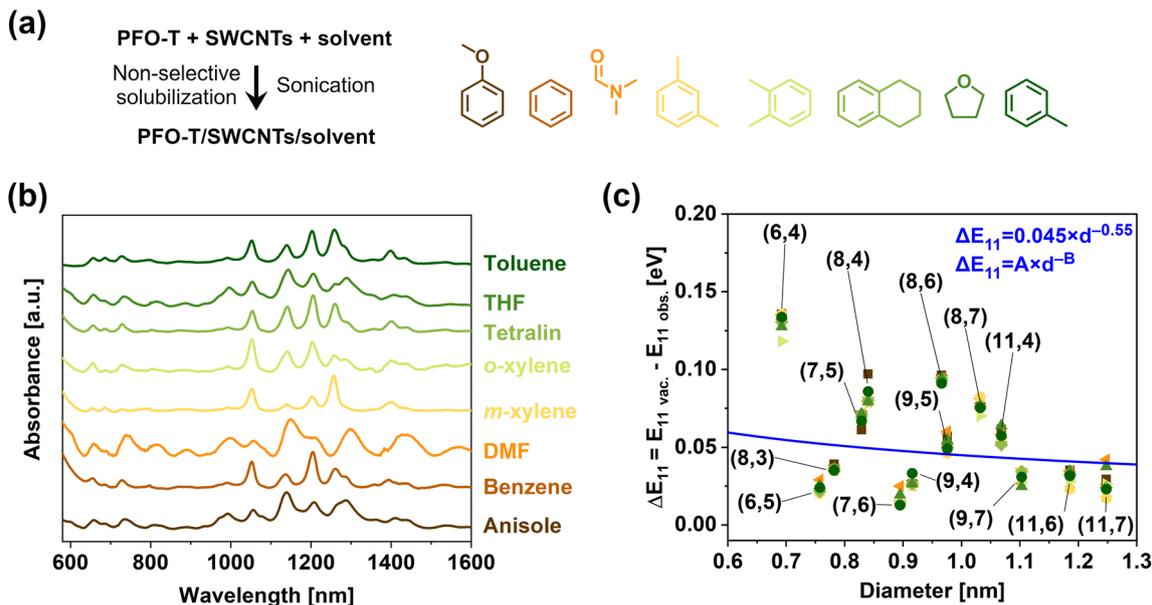
Fig. 3 (a) Employed methodology and solvents to study the optical properties of non-selectively solubilized HiPco SWCNTs. (b) Offset absorption spectra of SWCNTs individualized in various solvents by PFO-T. (c) Solvatochromic shifts as a function of solvent and SWCNT type calculated with respect to E_{11} positions determined for vacuum. The blue line represents the trend determined by Chuang *et al.* after the adjustment of $\Delta E_{11} = A \cdot d^{-B}$ function parameters to $A = 0.045$, $B = 0.55$, which gave the most accurate fitting.[51]

differentiation of HiPco SWCNTs are provided for comparison). The resulting optical absorption data were then deconvoluted, and the calculated composition of these materials was plotted as Sankey diagrams (Fig. S7b–e†). Extraction of SWCNTs in benzene and toluene using PFO exemplified how large the influence of the solvent on the extraction process may be. In toluene, mainly (7,5) SWCNTs were suspended, while extraction conducted in benzene produced a sample rich in the much smaller (6,4) SWCNTs. Therefore, drawing credible conclusions about solvatochromism without taking this issue into account is impossible, as the precision and accuracy of spectral deconvolution would greatly suffer because of this problem. Furthermore, the application of non-selective PFO-T led to the statistical solubilization of SWCNTs as expected, so the (6,5)-enriched SWCNT material contained (6,5) SWCNTs as the major species. The presence of other SWCNT chiralities should also be noted, as, contrary to what the trade name may suggest, this raw material contains many SWCNT types. Therefore, PFO-BPy had to be employed for further experiments instead of PFO-T, as the former polymer exhibited a much higher affinity toward (6,5) SWCNTs. In addition, PFO was employed to provide (7,5) SWCNTs for analysis.

Our methodology was designed to circumvent the issue of producing SWCNT fractions of considerably different compositions in different solvents. Maintaining the population distribution of isolated SWCNTs (as much as possible) after extraction was necessary to enable precise investigation of the solvatochromic effect, as the registered shifts were often minor. Knowing that the reliability and reproducibility of the selectivity exhibited by PFO-BPy and PFO were high, we decided to carry out several isolation processes in parallel to generate highly enriched fractions of (6,5) and (7,5) SWCNTs (Fig. S8†). A detailed side-by-side comparison of the obtained results from absorption spectroscopy and deconvolution of the obtained spectra (Fig. S9†) confirmed that these separation routines gave robust results. Such high performance in terms of both efficiency and selectivity was expected to be due to the significant difference in the binding energies of selectively wrapped (6,5) and (7,5) by PFO-BPy and PFO, respectively, compared to typical binding energies for the other chiralities coated by the same polymers.[54] Most of the remaining SWCNT types covered with these selective polymers precipitated during centrifugation. Still, the resulting suspensions always suffered some degree of contamination with polymer/SWCNT hybrids resembling the preferred chirality. In the case of PFO-BPy and PFO-dispersed SWCNTs in toluene, we estimated that the purity of the (6,5) and (7,5) species were 90.4% and 81.4%, respectively (Fig. S7 and S9†). Unfortunately, the lack of total selectivity of these polymers is commonly neglected in the literature. The samples generated using these polymers are regarded as monochiral, somewhat distorting the results of the studies based on them. This problem is often caused by overreliance on excitation–emission photoluminescence maps, which are more sensitive to detecting small-diameter SWCNTs due to their relatively bright photoluminescence.[62] Thus, we strongly suggest the collection and deconvolution of absorption spectra to discern the contribution of the individual species.

Following the isolation in toluene, the supernatants rich in (6,5) and (7,5) SWCNTs were divided into six new vials, accord-
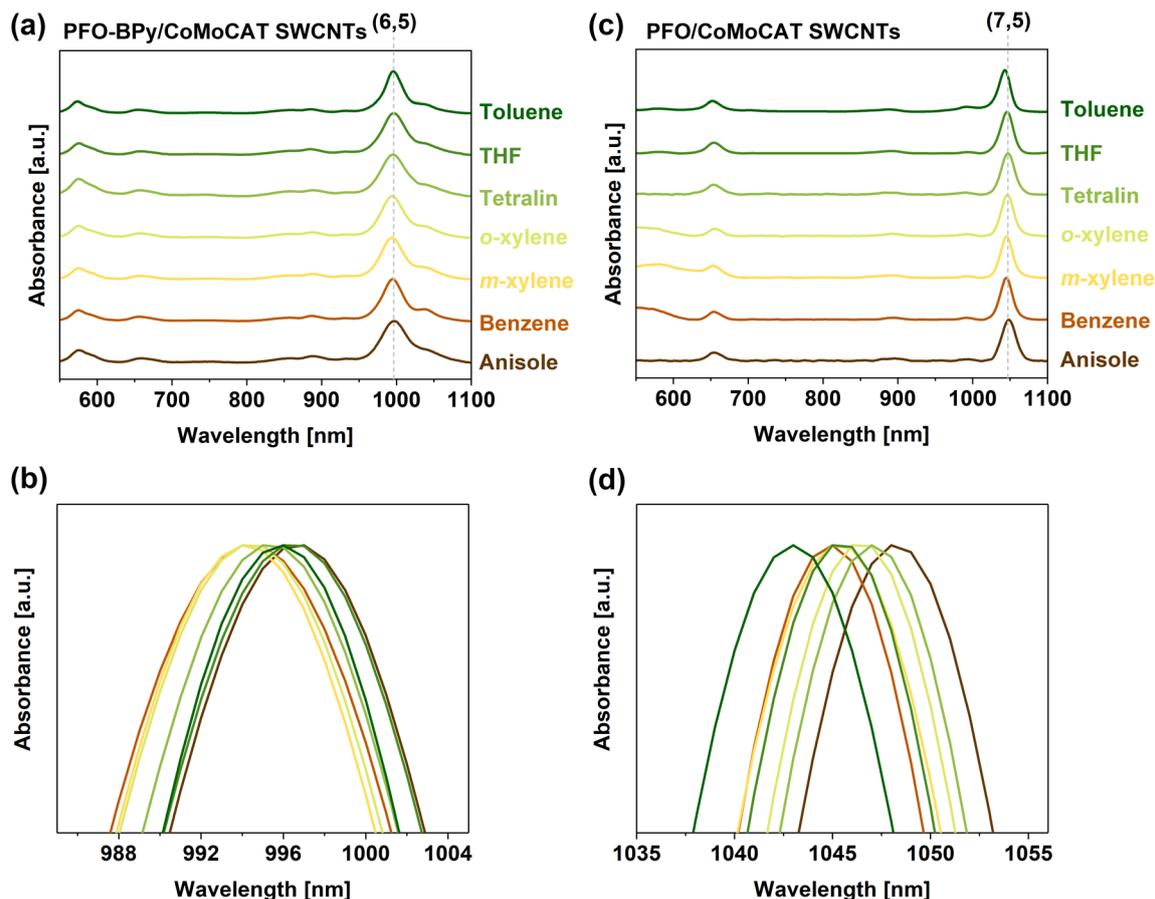
Fig. 4 (a) Offset absorption spectra of (6,5)-enriched SWCNTs solubilized in toluene using PFO-BPy and then redispersed in specified solvents. (b) Comparison of peak maxima positions of deconvoluted S_{11} optical transitions of (6,5) SWCNTs. (c) Offset absorption spectra of (7,5)-enriched SWCNTs solubilized in toluene using PFO and then redispersed in specified solvents. (d) Comparison of peak maxima positions of deconvoluted S_{11} optical transitions of (7,5) SWCNTs.

ing to the scheme shown in Fig. S8,† and used in subsequent experiments. Each of these supernatants was left to evaporate spontaneously. When this occurred, one of the selected solvents, *i.e.*, benzene, *m*-xylene, *o*-xylene, tetralin, tetrahydrofuran, or anisole, was added to each of them. The samples were then redispersed by sonication and remeasured using absorption spectroscopy (Fig. 4).

3.5. Elaboration of the mechanism of solvatochromism in polymer-suspended SWCNTs

We observed red shifts of the characteristic transitions, which were more pronounced in the case of (7,5) wrapped by PFO than for (6,5) SWCNTs suspended by PFO-BPy. The higher resistance to the solvent effect revealed in the case of (6,5)-chirality may be due to the greater ability of the layer formed by PFO-BPy to provide dielectric shielding of the SWCNTs. This disparity can be explained by the positions of the valence and conduction bands for the respective polymers, which allow for energy transfer in the case of P3HT/(7,5) SWCNT nanocomposites *via* type II heterojunctions,[54] as well as in special cases of type I for PFO-BPy/(6,5) SWCNT, according to the

mechanism described by Buckup *et al.*[39,63,64] This energy transfer phenomenon was reported several years earlier by Nicholas *et al.* for F8BT/(7,5) SWCNTs[54] and by Nakamura *et al.* for PFO/(7,6) SWCNTs.[65] Interestingly, for PFO/(7,5) SWCNTs, no such possibility has been observed so far. Thus, considering the lack of charge transfer, the interaction between PFO and (7,5) SWCNTs is not as strong as in the case of (6,5) SWCNTs and PFO-BPy, so (7,5) SWCNTs can be more readily affected by solvent molecules.

The increasing binding strength of SWCNTs follows the given sequence PFO < F8T2 – F8BT < P3HT,[54] corroborating the above deductions. Therefore, the reported relationship confirms that the PFO molecules bind rather weakly to SWCNTs, and thus their desorption may enable the solvent to access the SWCNT sidewall more easily. This claim is supported by the fact that the peak positions can be tuned in a reproducible manner when the solvent is changed (Fig. S10†).

Although, in recent years, the use of CPs for both selective and non-selective solubilization has come back into favor due to the substantial application of SWCNT suspensions in organic solvents, the topic of solvatochromism in such

systems seems to be inadequately debated, particularly considering that it is erroneous to believe that it is sufficient to transfer the relationships previously identified for surfactants to understand its effect. Since the nature of CPs in the context of solvatochromism is far more strongly related to structure and conformation than in the case of surfactants, the underlying phenomena are highly intertwined. Among other reasons, this is caused not only by the complex mechanism of suspension, which we described in the introduction, but also by the existence of notable energy transfer between the SWCNTs and the CPs, which enables numerous applications in photonics.[6,11,66] Moreover, the formation of interactions over a much larger surface area relative to a single surfactant unit results in more pronounced and less obvious oscillations of binding energy with respect to the diameter or chiral angle of SWCNTs.[36] Unraveling this puzzle is not simplified by the fact that, in the case of polymers, there is no standardized scheme for analyzing the strength of solvatochromism expressed as ΔE_{ii}. In this regard, the authors define it commonly as:[21–24,33,36,67,68]

$$\Delta E_{ii} = E_{ii} - E_{ii}^{\text{Weisman}} \text{ or } \Delta E_{ii} = E_{ii}^{\text{Weisman}} - E_{ii} \quad (1)$$

$$\Delta E_{ii} = E_{ii} - E_{ii}^{\text{local reference}} \quad (2)$$

$$\Delta E_{ii} = E_{ii}^{\text{PFH-A}} - E_{ii}^{\text{PFO-BPy}} \text{ or } \Delta E_{ii} = E_{ii}^{\text{PFO-Py}} - E_{ii}^{\text{PFO-PFDD}} \quad (3)$$

$$\Delta E_{ii} = E_{ii} - E_{ii,\text{VAC}} \qquad E_{ii,\text{VAC}} = \frac{1241 \text{ eV nm}}{A_1 + A_2 d_t} + A_3 \frac{\cos(3\theta)}{d_t^2} \quad (4)$$

In the first approach (eqn (1)), the measured transition energy is compared to the transition energies determined by Weisman *et al.*, who suspended SWCNTs with SDS surfactant in water[43] (care is needed because sometimes the position of references in the formula is switched causing the calculated shifts to appear with an inverted sign). This approach has considerable utility due to the wide range of reported chiralities and general recognition and appreciation in the community. However, in this case, we need to remember that the absolute strength of solvatochromism cannot be calculated this way because the measured shift is compared to already shifted transition energies (the microenvironment in the case of SDS/water dispersion does not fulfill the requirement of $\varepsilon = 1$). Furthermore, to eliminate uncertainty caused by different SWCNT dispersion protocols, some authors relate the measured results to the transition energies obtained independently using a locally prepared reference SWCNT suspension[67] (eqn (2)). This tactic also gives rise to relative quantification of the solvatochromic effect due to the same reason specified above. Alternatively, shifts are evaluated as a difference between the optical transitions of polymers suspending SWCNTs selectively and non-selectively (eqn (3)).[21,24] In this case, however, it is impossible to exclude the influence of the nature of the polymer reference (*e.g.*, molecular weight or conformation). Lastly, some literature sources compare the generated results against the expected positions of optical transitions for SWCNT in a vacuum (eqn (4)).[19,22,24]

The first three kinds of evaluations, unfortunately, do not allow for a straightforward comparison of results from different studies to quantify the solvatochromism effect between various groups of employed methods, CPs, or solvents. Therefore, in our investigation, we engaged the most direct reference, which is the comparison of the transition energy of each chirality to its calculated equivalent in a vacuum according to the methodology and the model introduced by Strano and Choi,[19] later successfully applied by Larsen *et al.*[23] and Ju *et al.*[22] (eqn (4)).

To determine the effect of CPs on the solvatochromism of SWCNTs suspended in various organic solvents, we first need to outline the current state of knowledge derived mainly from studies of surfactants or oligomers, and afterward extend this discussion to polymer-specific effects, such as the ability to induce mechanical stresses. This will aid a better understanding of the role of the individual constituent and clarify how the structural features of a polymer can affect changes in electronic and strain levels. In this context, the chemical structure of the polymer and its susceptibility to solvent-induced conformational changes are crucial, as they translate to the ability to form polymer-SWCNT interactions. They, in turn, affect the observed shift in the characteristic absorption or fluorescence bands of SWCNTs, the strength of which depends on two cumulative effects according to the equation $\Delta E_{11} = \Delta E_{\text{electronic}} + \Delta E_{\text{strain}}$.[33] Unfortunately, the literature mainly discusses the former effect, which results directly from the contribution of the dispersing agent and solvent to dielectric shielding (microenvironment effect). However, the importance of the latter aspect should also be appreciated.

A detailed theoretical description of the entire dielectric shielding phenomenon, together with modeling of its influence on solvatochromism effects, is included in a study by Miayauchi *et al.*[49] Particularly helpful in elucidating the role of either the dispersing agent or the solvent is the postulate that the SWCNT environment can be estimated by two simple parameters. The external medium is described by k_{env}, which is the static dielectric constant of the environment (that is the sum of the contributions of the solvent and the dispersing agent), and the internal medium ($k_{\text{tube}}^{\infty} - k^{\text{vac}}$), whose change is proportional to the change in SWCNT diameter in the expression $1/d_t^2$. The modeling carried out for a wide range of dielectric constants and different SWCNT diameters led to an important conclusion, which is the existence of a maximum possible shift, which is reached when $k_{\text{env}} \to \infty$. The magnitude of this shift is not the same for all chiralities, nor does it change linearly with respect to the diameter or chiral angle. In fact, it was observed that it strongly depends on the membership of SWCNTs to a particular family, defined as ($2n + m$ = const) and $n - m = 3p + q$ where p is an integer ($q = 1$ or 2 for semiconducting SWCNTs)[17,21,22,24,33,51,69].

Insights into these intricate correlations related to solvatochromism are crucial for extending the already developed theoretical models for the simpler surfactant-SWCNT systems. Even though during the early phase of studies on CPE, it was stated that the contribution of the solvent to the solvatochro-

mism effect was below the detection threshold,[36] thanks to the development of new instrumentation, in the following years there have been a few papers that have been able to observe it.[21,23] Unfortunately, the literature reports covered only a narrow scope of polymers and solvents, i.e., toluene and xylene for PFO-Py and PFDD,[21] as well as several other solvents for the PNES conjugated ionic polymer.[23] Given the complexity of the process and the multitude of interdependent structural effects, these results are insufficient to draw any general conclusions. It is also important to note that to consider the impact of solvent on organic SWCNT dispersions, it is currently necessary to rely on findings from surfactant-related studies, which, as we will show, is inadequate.[18,20,22,25]

Since absorption spectroscopy has a higher measurement resolution, we were able to quantify small variations in the position of the E_{11} absorption maxima, typically ranging from a few to several nm, driven by a change in the dielectric constant of the solvents, for a broad spectrum of chiralities (Fig. S11†). Nonetheless, no clear correlation could be discerned using this data. Similarly, attempts to relate ΔE_{11} (calculated with respect to vacuum) and the dielectric constants of the employed solvents were unsuccessful (Fig. S12†).

Before discussing the role of CP and solvent in detail using other parameters, we need to redefine several terms, which, if misinterpreted, can lead to confusion and erroneous conclusions. Seeking an answer to the first of the questions regarding the parameter describing the strength of the solvent solvatochromic effect defined as ΔE (change in transition energy), we should clarify what is hidden beneath this term. In the case of an empirical study of the solvatochromism effect, we cannot experimentally separate the individual types of interactions between the solvent and the solute, which in this case is a nanocomposite composed of a CP and SWCNT (not just SWCNTs). Thus, the description of the total solvation capacity of the solvent should take into account all possible non-specific and specific forms of interaction between the solvent molecules and the SWCNT/polymer hybrid, which are, respectively, coulombic, directional, induced, and dispersive interactions, as well as specific hydrogen bond donor–acceptor, electron pair donor–acceptor, and solvophobic interactions.[70]

In the referred study, one can find that among the numerous relationships identified, the most popular one describing how a change in dipole moment correlates with electron excitation and emission is the difference in the position of the maxima of absorption and fluorescence peaks. This relationship is usually presented as a function of solvent polarity, customarily based on the relative permittivity ε_r and the refractive index of the medium η.[70] These correlations based on Onsager's reaction-field theory were employed by Silvera-Batista et al. in their study.[25] These authors investigated the dependence of the shift of characteristic bands from SWCNTs suspended by SDBS in water after being placed in micelles containing organic solvents. The observed solvatochromic shifts were found to depend on the dielectric constant and induced polarizability $f(\eta^2) = 2(\eta^2 - 1)/(2\eta^2 + 1)$ of the solvent.

Similarly, locally functionalized surfactant-suspended SWCNTs in water, to which organic solvents were injected, were used to give a correlation of the solvatochromic effect with the solvent orientational polarizability derived from the formula $\Delta f = f(\varepsilon) - f(\eta^2)$, for which the previously calculated component of the induced polarizability, i.e., $f(\eta^2)$,[20] was subtracted from the total polarizability $f(\varepsilon) = 2(\varepsilon - 1)/(2\varepsilon + 1)$.

Finally, the last attempt to understand the effects of SWCNT solvatochromism mentioned here, which was the first to focus on polymers, was the study of Larsen et al.,[23] based on the PNES ionic polymer and SWCNT suspensions prepared using this polymer in polar solvents, e.g., MeOH, DMSO, D_2O, or D_2O : DMF. The authors concluded that the shift could be represented by the following equation:

$$\Delta E_{ii} E_{ii,VAC}{}^3 = -D_{SWNT/solvent}[f(\varepsilon) - f(\eta^2)](1/d^5) \qquad (5)$$

where $D_{SWNT/solvent}$ describes the interactions between the SWCNTs and the solvent. It was thus revealed that the SWCNT diameter appeared to be an important parameter to consider.

The peak positions determined after spectral deconvolution, shown in Fig. 3 and 4 for non-selectively- and selectively extracted SWCNTs, respectively, were converted to E_{11} transition energies (eV) to compare with the literature results presented above. The $E_{11,VAC}$ values were then calculated for each chirality using the formula from eqn (4).[71] Based on these data, it was possible to calculate E_{11} as the difference between the experimental value and the one estimated in a vacuum. The $f(\varepsilon)$ and $f(\varepsilon)$–$f(\eta^2)$ values calculated based on the formulas mentioned above were compiled in Table S1† and subsequently plotted versus calculated ΔE_{11} (Fig. S13 and S14†). Examining the data, it can be noted that they do not resemble the relationships determined by Silvera-Batista et al., Shiraki et al., or Niidome et al. for microenvironments containing organic solvents in micelles formed by surfactants,[18,20,25] which displayed a linear decrease with increasing ε,[14,17,23,25] $f(\eta^2)$,[25] or $f(\varepsilon) - f(\eta^2)$.[18,20] Likewise, for SWCNTs wrapped by flavin, a roughly linear decrease in the value of the solvatochromic shift with a logarithmic increase in ε was observed for most chiralities.[22] This relationship was also invalid for our systems. In contrast, we noted that the measure of solvatochromic effects, regardless of the parameter selected on the X-axis, usually oscillated in a range up to 10 or 20 meV, without any clear trend. Apart from us, the non-monotonic behavior of E_{11} with respect to the increasing static dielectric constant of the surroundings was demonstrated experimentally previously, despite the model itself predicting an exponential decrease for each SWCNT to a chirality-specific value.[49]

To tackle this problem further, we plotted the values of ΔE_{11} vs. SWCNT diameter to verify the previously reported higher sensitivity of small-diameter SWCNT to solvatochromic effects (Fig. 3c, cf. blue line) in surfactant-suspended SWCNTs.[51] While the data points were somewhat scattered, we also observed that ΔE_{11} was higher for small diameter SWCNTs, even though the PFO-T used in this study to disperse SWCNTs was uncharged (the relationship determined in the

Paper

cited study required parameter adjustment to model our system, *cf.* caption to Fig. 3). Unfortunately, because of a lack of consensus in the determination of ΔE_{11}, it was not possible to make a quantitative comparison of our results to the previous papers focusing on the topic of CPs and organic solvents.[24] Nonetheless, from a qualitative perspective, the E_{11} we determined for PFO-T was marginally higher than the values registered for the previously mentioned PNES used to solubilize SWCNTs in polar solvents,[23] ranging from 0.01 to 0.10 eV.

Furthermore, a review of the literature data reveals that scientists have invested a lot of time searching for an equation describing the polarizability of SWCNTs. They have proposed several different functional forms, most of which can be reduced to the general assumption $\alpha \sim R^a E^b$ in which R is the radius of the SWCNT (or D as a diameter), E is the optical band gap, and a, b are scaling parameters.[19,23,25] Some variations between them arise from the choice of the specific model and suspending protocol used, while the scaling parameters typically range from -1 to 2 and -3 to 0 for the para-

meters a and b, respectively.[19,23,25] Considering the similarities in methodology, *i.e.*, solubilization of SWCNTs *via* CPE, together with the same method of determining E_{11}, as the most relevant reference for our results, we considered the study conducted using PNES, in which shifts of optical transitions were gauged using eqn (5) shown above.[23]

Fig. 5a depicts our results from HiPco SWCNTs/PFO-T in toluene, along with the trend for water and methanol determined in the abovementioned paper. Unfortunately, the data generated by us did not follow these trends (and also those results previously described for surfactants[19,25]) as the CPs that wrapped around the SWCNTs were uncharged. Because the microenvironment has a key influence on the polarizability of SWCNTs, it seems that an ionic polymer such as PNES mirrors the behavior and correlations previously observed for surfactants such as SDS, SDBS, or SC due to its charged nature. Therefore, our problem remained unresolved.

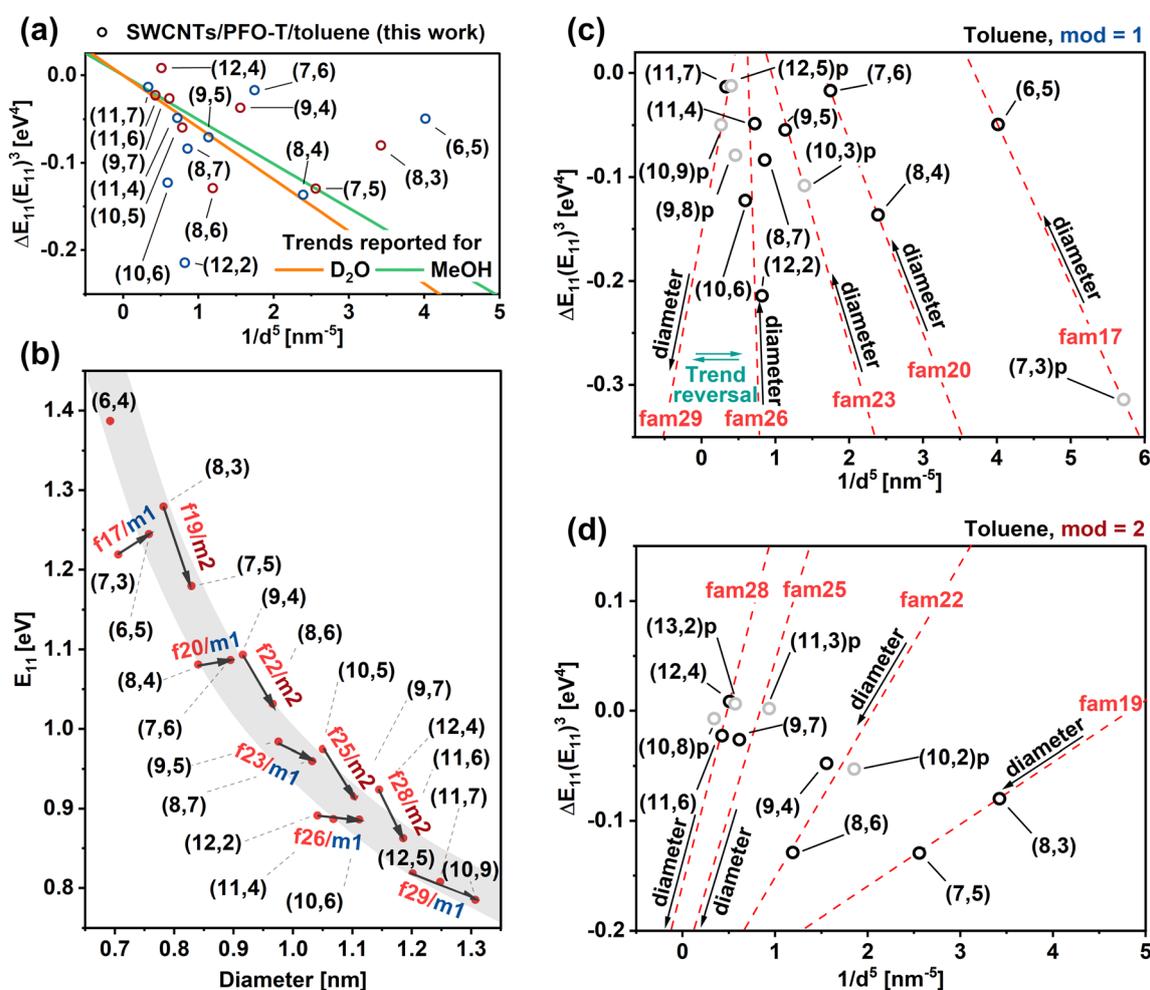Considering the foregoing, we decided to evaluate the possibility of the previously mentioned, but typically dis-

Fig. 5 (a) Unsuccessful attempt to model data from Fig. 3b and c according to eqn (5). Trend lines obtained from ref. 24. (b) Energy of E_{11} transitions plotted as a function of SWCNT diameter. Family and mod patterns annotated with *f*, *m*1/*m*2, respectively. (c) and (d) Data from Fig. 5a divided into mod 1 and 2, respectively. Family pattern for each chirality calculated according to $(2n + m)$ were marked with dashed lines to guide the eye.

regarded, strain induction described as ΔE_{strain} being the missing piece of this puzzle, which might explain the observed peculiarities. Although it was wholly overlooked in the previously discussed studies related to surfactants, its importance was reported for the dispersion of SWCNTs with porphyrin oligomers and for the growth of SWCNTs on pillars or trenches.[13,14,33] Its limited relevance for some systems probably stems from the fact that several planes of interaction between SWCNTs and an individual dispersant must be formed to produce shape-deforming stresses. While it is unlikely that surfactant molecules could noticeably affect the SWCNTs' shape, the polymer's rigidity should be sufficient to deform SWCNTs. Such a phenomenon can occur in the case of oligomers or polymers for which each monomer moiety forms an individual plane of interactions, much stronger than the typically investigated relationship of a single surfactant molecule with the SWCNT surface.[33]

In addition, SWCNTs can be classified into families (defined as the residual from equation $(n − m)$). In turn, these families react differently to uniaxial or radial deformation,[15] contributing variously to the solvatochromic effect. Considering the concept of SWCNT families, we observed certain periodic regularities that can quantify how the suspension of the specific SWCNTs in toluene gives rise to a solvatochromic shift. Each SWCNT type detected in the material was assigned a point reflecting its chirality, the corresponding mod, and the family (Fig. 5b).

To deepen the analysis, we separated the mods from each other and listed them in separate graphs (Fig. 5c and d). For some families, fam = 29, 23, 17, due to the lack of sufficient numbers of identified chiralities, it was necessary to rely on the literature data of the mean peak positions given in Fig. 2 and Table S3† to mark the unrecognized SWCNTs in the plots (denoted with p for predicted) and hence estimate the plausible trend line (marked as a dashed line). Even if it was not essential to improve the model's reliability, we proceeded analogously for the remaining families. In summary, we estimated the position and added to the graph the following chiralities: (13,2), (12,5), (11,3), (10,9), (10,8), (10,3), (10,2), (9,8), and (7,3). The distinct nature of SWCNTs classified as mod = 1 and mod = 2 was clearly visible. For the latter group, we observed that the sensitivity to the solvatochromism effect increased as the diameter increased (higher absolute value of $\Delta E_{ii}E_{ii,VAC}$). Surprisingly, polymer-wrapped SWCNT behavior was strongly dependent on the assignment to the individual families since the change in the slope of the trend lines was evident. Conversely, for the first group, i.e., mod = 1, the effect was reversed, and as the diameter increased, the absolute value describing the discussed quantity decreased. The mentioned change in the slope occurred here between fam = 26 and 29. A deviation from the previously estimated pattern could be seen for fam = 29, for which the slope became similar to mod = 2, although these SWCNTs belonged to mod = 1.

To explain this previously unobserved, unique relationship of SWCNTs wrapped with CPs, we need to refer to the stress induction ΔE_{strain} discussed earlier and its impact on the shift

of ΔE_{11}. Given that the strain component for mod = 2 ($q = −1$) was negative, and for mod = 1 ($q = 1$) was positive,[33] we postulate the hypothesis of constructive interference of both effects $\Delta E_{11\ electronic} + \Delta E_{11\ strain}$ in the case of SWCNTs classified as mod = 2. In contrast, for mod = 1, due to the positive value of $\Delta E_{11\ strain}$ and negative value of $\Delta E_{11\ electronic}$, there is mutual suppression (extinction) of both effects. The trend reversal for fam = 29 was deduced using the position of the estimated $\Delta E_{ii}E_{ii,VAC}^{3}$ value calculated for the (10,9)-chirality based on literature data, as this SWCNT type was not detected in our material. This oddity can be justified by the relationship determined by Stranks et al.,[33] who reported that the magnitude of the $E_{11\ strain}$ tended toward 0 as the chiral angle increased. Notably, (10,9)-chirality had the highest chiral angle out of all the SWCNT types presented in the graph, which may mean that the strain component was smaller for this chiral type than for the other SWCNTs probed. This could have resulted in the suppression effect of both components eventually becoming negligible, and thus the fam = 29 family began to behave like fam = 25 and 28, which were of a different mod.

The pattern evolution process for mod = 1 is clearly visible in Fig. 5b by considering the transition energy E_{11} plotted against the diameter of SWCNTs. Contrary to published reports, we can see that although the relationship appeared to be linear for the individual families, the overall correlation was non-linear across all the evaluated SWCNT types. The decrease in the value of E_{11} for mod = 1 followed the order of families in the sequence fam = 17 → 20 → 23 → 26 → 29 (the characteristic transition energy E_{11} changed only slightly within individual families). Besides, the directional coefficient of the predicted trend lines also gradually changed from positive to negative values between families 17 and 29 in the case of mod = 1. The change in slope for mod = 2 was much less apparent.

In essence, when analyzing only the whole picture without considering the behavior of individual mods or families, it appears that SWCNTs show an exponential relationship between the transition energy E_{11} and the diameter. Instead, the correlation is not so straightforward, as different SWCNT classes exhibit distinct behavior. The discovery of this relationship strongly supports our hypothesis that complex solvatochromic shifts in polymer-suspended SWCNTs are strongly affected by the strain effect, which is experienced dissimilarly by SWCNTs of various families and mods. The findings reported herein are in agreement with the theoretical model developed by Yang and Han[72] who showed that optical properties of SWCNTs are influenced by mechanical deformation of the material. Depending on whether the deformation is uniaxial or torsional, and whether it leads to compression or stretching of the SWCNT, the band gaps of particular SWCNT types are affected differently. Hence, diameter and chiral angle of SWCNTs are important factors to consider in this context. For instance, the band gap of (10,10) SWCNTs is only slightly modified when subjected to uniaxial strain, but torsional strain impacts it substantially. Finally, the results of simulations also confirm that SWCNTs of different mod values may exhibit contrasting behavior, validating the interpretation of the experimental results obtained by us.

4. Conclusions

In this paper, we have shown that the solvatochromic effect in SWCNTs extracted by conventional conjugated homopolymers based on fluorene and its co-polymers with thiophene or bipyridyl present a distinct nature compared to literature reports based on the solubilization of SWCNTs with ionic surfactants or ionic polymers. This is manifested not only in the strong red shifts of the optical transition peaks, but also in these shifts exhibiting non-monotonic evolution with respect to the tube diameter. The discussed phenomenon heavily depends on the chirality of isolated SWCNTs, the microenvironment created by the solvent, and especially on the choice of wrapping CP. The results suggest that it is likely the consequence of the decisive influence of the polymer's structure on the occurrence of striking differences in its electron properties (HOMO/LUMO energy, bandgap), established conformations, and the ability to form interactions with the surface of the SWCNT. Furthermore, the rather rigid conformation of the CPs makes them quite selective regarding affinity to specific ranges of diameters or chiral angles and, more broadly, for particular families. Compounding the issue is the existence of charge transfer between the polymer and the SWCNTs, which hinges on the orbitals overlapping with certain SWCNT types. The mentioned elements are reflected in the complex and so far unexplored mechanism of selective CPE. It is caused by multiple kinds of interactions within the SWCNT-polymer-solvent system leading to non-monotonic evolution of both constituents, defining the strength of the optical transition shift, namely $\Delta E = \Delta E_{\text{electric}} + \Delta E_{\text{strain}}$. However, as we have shown, certain regularities can be revealed in this area by assigning isolated SWCNTs to different mods and families.

To precisely elucidate the behavior of such a complex system, we examined how a broad spectrum of chiralities responds to extraction with CPs, *i.e.*, PFO-T, PFO, and PFO-BPy. Subsequently, we conducted an in-depth analysis of the literature data along with selecting, in our opinion, the most reliable methodology to determine the solvatochromism effect. To obtain a comprehensive amount of experimental data, a robust analysis protocol was built based on the use of an efficient, but non-selective, CP with a high tolerance to organic solvents, *i.e.*, PFO-T.

To contrast the role of the CP with that played by the solvent, the strength of solvatochromism for polymers that demonstrated selective isolation capabilities but differed in structure, *i.e.*, PFO and PFO-BPy, was investigated. To conduct this analysis, a new methodology was proposed. It facilitated the complex process of deconvolution of absorption spectra from SWCNTs by stabilizing the composition of the studied system. Thus, it was possible to observe shifts in optical transitions for different microenvironments, which were more pronounced for PFO-wrapped (7,5) SWCNTs than for the (6,5)-chirality suspended by PFO-BPy.

Furthermore, the paramount aspect of this contribution was the elucidation of correlations describing the evolution of the solvatochromism effect strength. Firstly, we looked at the dependency of the optical shift on the change of common parameters describing organic solvents, including the dielectric constant, and the induced or oriented polarizability. Unfortunately, regardless of the chosen parameter, the observed solvatochromism effect ranged up to 10 or 20 meV for most SWCNT chiralities and CPs without any clear trend. This may be due to the two effects offsetting each other, *i.e.*, a more polar solvent leads to a higher redshift but softens the polymer chain, which may weaken its interaction with the SWCNT surface, thus reducing the redshift.

A breakthrough was achieved once the $\Delta E_{\text{ii}} E_{\text{ii,VAC}}{}^3$ was plotted as a function of $(1/d^5)$ and investigated in detail. A complete picture of solvatochromism of polymer-suspended SWCNTs in organic solvents encompassing a plethora of chiral types from different starting materials was accomplished as a result. The novelty of this work lies in the elaboration of the considerable impact of mods on the optical properties of SWCNTs suspended in organic solvents using CPs. To the best of our knowledge, this is the first paper that not only reports such dependencies but also provides a plausible explanation of what causes the observed hierarchical and periodic behavior. It should be noted that these relationships are markedly different from those previously observed for surfactants and ionic polymers, which indicate that for these cases solvatochromism depends mainly on electronic effects, *i.e.*, the ability of the surfactant molecules to polarize the SWCNT and shield it from the influence caused by solvent. In contrast, due to the unique interactions between polymers and SWCNTs, it is the strain that determines the magnitude of a solvatochromic shift instead of the electronic effects.

In the case of SWCNTs representing mod = 1, as the diameter increased, the absolute value of $\Delta E_{\text{ii}} E_{\text{ii,VAC}}{}^3$ decreased. For mod = 2, this trend was opposite, most likely due to the mutual amplification of the negative electronic effect of the $\Delta E_{\text{electric}}$ and ΔE_{strain} coefficient. On the other hand, for mod = 1 the electronic contribution was negative, while the strain effect was positive, which resulted in a weakening of the dielectric shielding. Interestingly, this trend was reversed for the family = 29, belonging to mod = 1, due to the very high value of the chiral angle for the chirality (10,9), resulting in the marginalization of the strain component and the emergence of mod = 2-like behavior. We hope that the newly discovered relationships will facilitate a greater understanding of the optoelectronic characteristics of materials at the nanoscale.

Conflicts of interest

There are no conflicts of interest to declare.

Acknowledgements

References

1 E. Bekyarova, M. E. Itkis, N. Cabrera, B. Zhao, A. Yu, J. Gao and R. C. Haddon, *J. Am. Chem. Soc.*, 2005, **127**, 5990–5995.

2 Z. Yao, C. C. Zhu, M. Cheng and J. Liu, *Comput. Mater. Sci.*, 2001, **22**, 180–184.

3 J. Zaumseil, *Adv. Opt. Mater.*, 2022, **10**, 2101576.

4 A. S. R. Bati, L. Yu, M. Batmunkh and J. G. Shapter, *Nanoscale*, 2018, **10**, 22087–22139.

5 C. T. White and J. W. Mintmire, *J. Phys. Chem. B*, 2005, **109**, 52–65.

6 X. He, N. F. Hartmann, X. Ma, Y. Kim, R. Ihly, J. L. Blackburn, W. Gao, J. Kono, Y. Yomogida, A. Hirano, T. Tanaka, H. Kataura, H. Htoon and S. K. Doorn, *Nat. Photonics*, 2017, **11**, 577–582.

7 X. He, H. Htoon, S. K. Doorn, W. H. P. Pernice, F. Pyatkov, R. Krupke, A. Jeantet, Y. Chassagneux and C. Voisin, *Nat. Mater.*, 2018, **17**, 663–670.

8 S. Kruss, A. J. Hilmer, J. Zhang, N. F. Reuel, B. Mu and M. S. Strano, *Adv. Drug Delivery Rev.*, 2013, **65**, 1933–1950.

9 S. Bhattacharya, X. Gong, E. Wang, S. K. Dutta, J. R. Caplette, M. Son, F. T. Nguyen, M. S. Strano and D. Mukhopadhyay, *Cancer Res.*, 2019, **79**, 4515–4523.

10 R. Nißler, O. Bader, M. Dohmen, S. G. Walter, C. Noll, G. Selvaggio, U. Groß and S. Kruss, *Nat. Commun.*, 2020, **11**, 5995.

11 D. Janas, *Mater. Horiz.*, 2020, **7**, 2860–2881.

12 D. Janas, *Mater. Chem. Front.*, 2018, **2**, 36–63.

13 J. Lefebvre, J. M. Fraser, Y. Homma and P. Finnie, *Appl. Phys. A: Mater. Sci. Process.*, 2004, **78**, 1107–1110.

14 Y. Ohno, S. Iwasaki, Y. Murakami, S. Kishimoto, S. Maruyama and T. Mizutani, *Phys. Status Solidi*, 2007, **244**, 4002–4005.

15 A. G. Souza Filho, N. Kobayashi, J. Jiang, A. Grüneis, R. Saito, S. B. Cronin, J. Mendes Filho, G. G. Samsonidze, G. Dresselhaus and M. S. Dresselhaus, *Phys. Rev. Lett.*, 2005, **95**, 217403.

16 P. Finnie, Y. Homma and J. Lefebvre, *Phys. Rev. Lett.*, 2005, **94**, 247401.

17 J. Campo, S. Cambré, B. Botka, J. Obrzut, W. Wenseleers and J. A. Fagan, *ACS Nano*, 2021, **15**, 2301–2317.

18 T. Shiraki, Y. Niidome, F. Toshimitsu, T. Shiraishi, T. Shiga, B. Yu and T. Fujigaya, *Chem. Commun.*, 2019, **55**, 3662–3665.

19 J. H. Choi and M. S. Strano, *Appl. Phys. Lett.*, 2007, **90**, 223114.

20 Y. Niidome, B. Yu, G. Juhasz, T. Fujigaya and T. Shiraki, *J. Phys. Chem. C*, 2021, **125**, 12758–12766.

21 M. Tange, T. Okazaki and S. Iijima, *Nanoscale*, 2014, **6**, 248–254.

22 I.-S. Choi, M. Park, E. Koo and S.-Y. Ju, *Carbon*, 2021, **184**, 346–356.

23 B. A. Larsen, P. Deria, J. M. Holt, I. N. Stanton, M. J. Heben, M. J. Therien and J. L. Blackburn, *J. Am. Chem. Soc.*, 2012, **134**, 12485–12491.

24 K. S. Mistry, B. A. Larsen and J. L. Blackburn, *ACS Nano*, 2013, **7**, 2231–2239.

25 C. A. Silvera-Batista, R. K. Wang, P. Weinberg and K. J. Ziegler, *Phys. Chem. Chem. Phys.*, 2010, **12**, 6990.

26 M. Rohlfing, *Phys. Rev. Lett.*, 2012, **108**, 087402.

27 F. Wang, M. Y. Sfeir, L. Huang, X. M. H. Huang, Y. Wu, J. Kim, J. Hone, S. O'Brien, L. E. Brus and T. F. Heinz, *Phys. Rev. Lett.*, 2006, **96**, 167401.

28 Y. Joo, G. J. Brady, M. J. Shea, M. B. Oviedo, C. Kanimozhi, S. K. Schmitt, B. M. Wong, M. S. Arnold and P. Gopalan, *ACS Nano*, 2015, **9**, 10203–10213.

29 S. Qiu, K. Wu, B. Gao, L. Li, H. Jin and Q. Li, *Adv. Mater.*, 2019, **31**, 1800750.

30 Y. Li, M. Zheng, J. Yao, W. Gong, Y. Li, J. Tang, S. Feng, R. Han, Q. Sui, S. Qiu, L. Kang, H. Jin, D. Sun and Q. Li, *Adv. Funct. Mater.*, 2022, **32**, 2107119.

31 J. Wang and T. Lei, *Polymers*, 2020, **12**, 1548.

32 D. Fong and A. Adronov, *Chem. Sci.*, 2017, **8**, 7292–7305.

33 S. D. Stranks, J. K. Sprafke, H. L. Anderson and R. J. Nicholas, *ACS Nano*, 2011, **5**, 2307–2315.

34 A. Nish, J.-Y. Hwang, J. Doig and R. J. Nicholas, *Nat. Nanotechnol.*, 2007, **2**, 640–646.

35 J.-Y. Hwang, A. Nish, J. Doig, S. Douven, C.-W. Chen, L.-C. Chen and R. J. Nicholas, *J. Am. Chem. Soc.*, 2008, **130**, 3543–3553.

36 T. Schuettfort, A. Nish and R. J. Nicholas, *Nano Lett.*, 2009, **9**, 3871–3876.

37 C. Pramanik, J. R. Gissinger, S. Kumar and H. Heinz, *ACS Nano*, 2017, **11**, 12805–12816.

38 J. Gao, M. A. Loi, E. J. F. De Carvalho and M. C. Dos Santos, *ACS Nano*, 2011, **5**, 3993–3999.

39 S. D. Stranks, C. K. Yong, J. A. Alexander-Webber, C. Weisspfennig, M. B. Johnston, L. M. Herz and R. J. Nicholas, *ACS Nano*, 2012, **6**, 6058–6066.

40 Origin Help - ALS Baseline, **https://www.originlab.com/doc/Origin-Help/PeakAnalyzer-ALSBaseline**, (accessed 14 November 2022).

41 Y. Maeda, Y. Konno, A. Nishino, M. Yamada, S. Okudaira, Y. Miyauchi, K. Matsuda, J. Matsui, M. Mitsuishi and M. Suzuki, *Nanoscale*, 2020, **12**, 6263–6270.

42 M. Pfohl, D. D. Tune, A. Graf, J. Zaumseil, R. Krupke and B. S. Flavel, *ACS Omega*, 2017, **2**, 1163–1171.

43 S. M. Bachilo, M. S. Strano, C. Kittrell, R. H. Hauge, R. E. Smalley and R. B. Weisman, *Science*, 2002, **298**, 2361–2366.

44 H. W. Lee, Y. Yoon, S. Park, J. H. Oh, S. Hong, L. S. Liyanage, H. Wang, S. Morishita, N. Patil, Y. J. Park, J. J. Park, A. Spakowitz, G. Galli, F. Gygi, P. H. S. Wong, J. B. H. Tok, J. M. Kim and Z. Bao, *Nat. Commun.*, 2011, **2**, 541.

45 F. A. Lemasson, T. Strunk, P. Gerstel, F. Hennrich, S. Lebedkin, C. Barner-Kowollik, W. Wenzel, M. M. Kappes and M. Mayor, *J. Am. Chem. Soc.*, 2011, **133**, 652–655.

46 P. Imin, M. Imit and A. Adronov, *Macromolecules*, 2012, **45**, 5045–5050.

47 N. A. Rice and A. Adronov, *Macromolecules*, 2013, **46**, 3850–3860.

48 N. A. Rice, A. V. Subrahmanyam, B. R. Coleman and A. Adronov, *Macromolecules*, 2015, **48**, 5155–5161.

49 Y. Miyauchi, R. Saito, K. Sato, Y. Ohno, S. Iwasaki, T. Mizutani, J. Jiang and S. Maruyama, *Chem. Phys. Lett.*, 2007, **442**, 394–399.

50 F. Toshimitsu and N. Nakashima, *Nat. Commun.*, 2014, **5**, 5041.

51 K.-C. Chuang, A. Nish, J.-Y. Hwang, G. W. Evans and R. J. Nicholas, *Phys. Rev. B: Condens. Matter Mater. Phys.*, 2008, **78**, 085411.

52 Z. Cao, M. Leng, Y. Cao, X. Gu and L. Fang, *J. Polym. Sci.*, 2022, **60**, 298–310.

53 L. A. Galuska, W. W. McNutt, Z. Qian, S. Zhang, D. W. Weller, S. Dhakal, E. R. King, S. E. Morgan, J. D. Azoulay, J. Mei and X. Gu, *Macromolecules*, 2020, **53**, 6032–6042.

54 S. D. Stranks, A. M. R. R. Baker, J. A. Alexander-Webber, B. Dirks and R. J. Nicholas, *Small*, 2013, **9**, 2245–2249.

55 H.-P. Hsu, W. Paul and K. Binder, *Macromolecules*, 2010, **43**, 3094–3102.

56 A. D. McNaught and A. Wilkinson, *The IUPAC Compendium of Chemical Terminology*, International Union of Pure and Applied Chemistry (IUPAC), Research Triangle Park, NC, 2019.

57 J. P. Aime, P. Garrin, G. L. Baker, S. Ramakrishnan and P. Timmins, *Synth. Met.*, 1991, **41**, 859–867.

58 F. Jakubka, S. P. Schießl, S. Martin, J. M. Englert, F. Hauke, A. Hirsch and J. Zaumseil, *ACS Macro Lett.*, 2012, **1**, 815–819.

59 H. Wang, B. Hsieh, G. Jiménez-Osés, P. Liu, C. J. Tassone, Y. Diao, T. Lei, K. N. Houk and Z. Bao, *Small*, 2015, **11**, 126–133.

60 D. Fong, W. J. Bodnaryk, N. A. Rice, S. Saem, J. M. Moran-Mirabal and A. Adronov, *Chem. – Eur. J.*, 2016, **22**, 14560–14566.

61 J. Ouyang, J. Ding, J. Lefebvre, Z. Li, C. Guo, A. J. Kell and P. R. L. Malenfant, *ACS Nano*, 2018, **12**, 1910–1919.

62 S. Ren, M. Bernardi, R. R. Lunt, V. Bulovic, J. C. Grossman and S. Gradečak, *Nano Lett.*, 2011, **11**, 5316–5321.

63 A.-M. Dowgiallo, K. S. Mistry, J. C. Johnson and J. L. Blackburn, *ACS Nano*, 2014, **8**, 8573–8581.

64 Z. Kuang, F. J. Berger, J. L. P. Lustres, N. Wollscheid, H. Li, J. Lüttgens, M. B. Leinen, B. S. Flavel, J. Zaumseil and T. Buckup, *J. Phys. Chem. C*, 2021, **125**, 8125–8136.

65 A. Nakamura, T. Koyama, Y. Miyata and H. Shinohara, *J. Phys. Chem. C*, 2016, **120**, 4647–4652.

66 S. Yamashita, Y. Saito and J. H. Choi, *Carbon nanotubes and graphene for photonic applications*, Woodhead Publishing Limited, 2013.

67 W. Yi, A. Malkovskiy, Q. Chu, A. P. Sokolov, M. L. Colon, M. Meador and Y. Pang, *J. Phys. Chem. B*, 2008, **112**, 12263–12269.

68 J. Ouyang, H. Shin, P. Finnie, J. Ding, C. Guo, Z. Li, Y. Chen, L. Wei, A. J. Wu, S. Moisa, F. Lapointe and P. R. L. Malenfant, *ACS Appl. Polym. Mater.*, 2022, **4**, 6239–6254.

69 T. Ando, *J. Phys. Soc. Jpn.*, 2010, **79**, 024706.

70 C. Reichardt and T. Welton, *Solvents and Solvent Effects in Organic Chemistry*, Wiley-VCH Verlag GmbH & Co. KGaA, Weinheim, Germany, 2010.

71 R. B. Weisman and S. M. Bachilo, *Nano Lett.*, 2003, **3**, 1235–1238.

72 L. Yang and J. Han, *Phys. Rev. Lett.*, 2000, **85**, 154–157.